

## Nitrogen-Rich Oligoacenes: Candidates for n-Channel Organic Semiconductors

Michael Winkler\*<sup>†</sup> and K. N. Houk<sup>‡</sup>

Contribution from the Institut für Organische Chemie, Universität Würzburg, Am Hubland, 97074 Würzburg, Germany, and Department of Chemistry and Biochemistry, University of California, Los Angeles, California 90095-1569

Received October 3, 2006; E-mail: winkler@chemie.uni-wuerzburg.de

**Abstract:** The successive replacement of CH moieties by nitrogen atoms in oligoacenes (benzene to hexacene) has been studied computationally at the B3LYP/6-311+G(d,p)//6-31G(d) level of theory, and the effects of different heteroatomic substitution patterns on structures, electron affinities, excitation, ionization, and reorganization energies are discussed. The calculated tendencies are rationalized on the basis of molecular orbital arguments. To achieve electron affinities of 3 eV, a value required to allow for efficient electron injection from common metal electrodes, at least seven nitrogen atoms have to be incorporated into tetracenes or pentacenes. The latter require rather small reorganization energies for electron transfer (<0.20 eV) making these compounds promising candidates for n-channel semiconducting materials. Particularly interesting are heptaazapentacenes **5** and **6** in which the nitrogen atoms are arranged to form self-complementary systems with a maximum number of intermolecular CH–N contacts in planar oligomers. These interactions are expected to facilitate the formation of graphite-like sheet structures with cofacial arrangements of the  $\pi$  systems and short interlayer distances due to attractive N–C(H) interlayer interactions. This should not only be ideal for charge transfer but also might contribute to improved air stability of these semiconductors. Self-complementarity is maintained in azaacenes containing two cyano groups in the terminal rings. These compounds require lower reorganization energies than the unsubstituted heterocycles (0.13–0.14 eV), show high electron affinities (3.3 eV), and are thus promising candidates for materials applications.

### Introduction

During the past decades there has been significant progress in the development and rational design of organic thin film transistors (OTFTs).<sup>1</sup> Most efforts have been devoted to semiconductors with p-type characteristics, whereas n-channel materials in which the majority carriers are electrons came into the focus of materials research more recently. The design of high-performance n-type materials is desirable for the fabrication of p–n junctions and complementary logic circuits. Frisbie, Bredas, and co-workers summarized the progress made in the field up to the summer of 2004.<sup>1f</sup> These authors also formulated design principles, i.e., necessary and desirable properties required for organic materials to be useful as n-channel semiconductors in OTFTs.

The overall performance of OTFT devices, measured in terms of charge-carrier mobility, on-to-off current ratio, and threshold

voltage, depends in a complex way on the intrinsic electronic properties of the semiconductor molecules, their spatial orientation (crystal structure), and the film morphology and crystallinity. The latter can to some degree be controlled by varying the deposition conditions during preparation of the films, whereas the former are accessible to crystal engineering and molecular design. Most single-molecule organic semiconductors are composed of extended  $\pi$ -conjugated systems. The availability of high-energy occupied and low-energy unoccupied molecular orbitals in these systems facilitates injection of holes or electrons from the source metal electrode into the semiconductor and subsequent extraction at the drain electrode. In addition, extended  $\pi$ -conjugated systems allow for effective intra- and intermolecular delocalization and transport of charge. Although the mechanisms of intermolecular charge transfer (band-like vs hopping) are often difficult to determine conclusively on the basis of measured temperature dependencies of mobilities alone, the charge transport in weakly bound (disordered)  $\pi$ -conjugated materials is usually thermally activated and, thus, limited by trapping processes. Apart from potential external traps (defects, impurities, grain boundaries) self-trapping can account for this behavior when the average residence time of a charge carrier on a specific molecule is similar in magnitude to the relaxation time of that molecule to the optimum geometry of the charged state. In that hopping regime the charge transfer

<sup>†</sup> Universität Würzburg.

<sup>‡</sup> University of California.

(1) Representative reviews: (a) Mitschke, U.; Bäuerle, P. *J. Mater. Chem.* **2000**, *10*, 1471. (b) Würthner, F. *Angew. Chem., Int. Ed.* **2001**, *40*, 1037. (c) Katz, H. E.; Bao, Z.; Gilat, S. L. *Acc. Chem. Res.* **2001**, *34*, 359. (d) Dimitrakopoulos, C. D.; Malenfant, P. R. L. *Adv. Mater.* **2002**, *14*, 99. (e) Bendikov, M.; Wudl, F.; Perepichka, D. F. *Chem. Rev.* **2004**, *104*, 4891. (f) Newman, C. R.; Frisbie, C. D.; da Silva, Filho, D. A.; Bredas, J.-L.; Ewbank, P. C.; Mann, K. R. *Chem. Mater.* **2004**, *16*, 4436. (g) Bredas, J.-L.; Beljonne, D.; Coropceanu, V.; Cornil, J. *Chem. Rev.* **2004**, *104*, 4971. (h) Würthner, F.; Schmidt, R. *Chem. Phys. Chem.* **2006**, *7*, 793. For a nice review about functionalized acenes and their application in organic electronics, see: (i) Anthony, J. E. *Chem. Rev.* **2006**, *106*, 5028–5048.

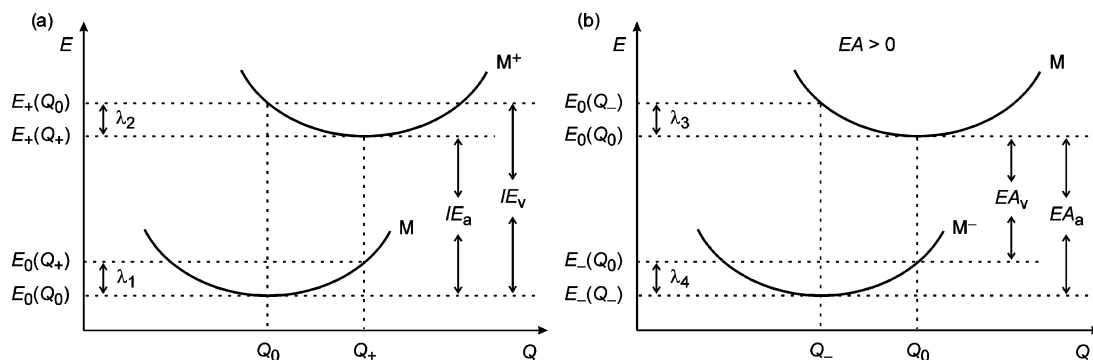


**Figure 1.** Definition of the internal reorganization energy for (a) hole transfer reaction  $M + M^+ \rightarrow M^+ + M$  and (b) electron-transfer reaction  $M + M^- \rightarrow M^- + M$ . The cation (anion) reorganization energy  $\lambda_2$  ( $\lambda_4$ ) is equal to the difference between the vertical and adiabatic ionization energy (electron affinity):  $\lambda_2 = IE_v - IE_a$  ( $\lambda_4 = |EA_v - EA_a|$ ).

can be described as a self-exchange electron-transfer reaction between a neutral molecule and a neighboring radical anion (n-type) or radical cation (p-type). The rate constants for electron transfer and, hence, the mobilities can then be modeled by classical Marcus theory,

$$k_{\text{et}} = (t^2/\hbar)(\pi/\lambda_{\pm} k_{\text{B}}T)^{1/2} \exp(-\lambda_{\pm}/4 k_{\text{B}}T) \quad (1)$$

where  $t$  is the transfer integral,  $\lambda_{\pm}$  is the reorganization energy,  $k_{\text{B}}$  is the Boltzmann constant, and  $T$  is the temperature.

The (inner) reorganization energies  $\lambda_{\pm}$  can be defined as shown in Figure 1. The reorganization energy  $\lambda_+$  ( $\lambda_-$ ) for hole (electron) transport is calculated as the sum of the energy required for reorganization of the vertically ionized neutral to the cation (anion) geometry,  $\lambda_2$  ( $\lambda_4$ ), plus the energy required to reorganize the cation (anion) geometry back to the neutral equilibrium structure on the ground state potential energy surface,  $\lambda_1$  ( $\lambda_3$ ).

$$\lambda_+ = \lambda_1 + \lambda_2 = E_0(Q_+) - E_0(Q_0) + E_+(Q_0) - E_+(Q_+)$$

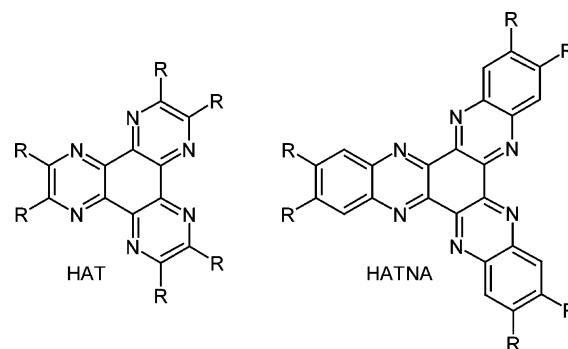
$$\lambda_- = \lambda_3 + \lambda_4 = E_0(Q_-) - E_0(Q_0) + E_-(Q_0) - E_-(Q_-) \quad (2)$$

The high charge carrier mobilities of oligoacenes, especially tetracenes and pentacenes, the archetypical p-type semiconductors, have been attributed largely to the small  $\lambda_+$  of these materials. Electronically, the small reorganization energies are a consequence of the completely delocalized nature of the frontier molecular orbitals that are spread out over the entire molecule so that ionization or capture of an electron do not lead to significant geometrical distortions.<sup>1</sup>

A small reorganization energy  $\lambda_-$  for electron transport is only one molecular property that an n-channel semiconductor should possess. To allow for efficient electron injection from common metal electrodes, the electron affinity ( $EA$ ) should be in excess of 3.0 eV.<sup>1f</sup> Most n-type semiconductors are derived from p-channel materials by introduction of electron-withdrawing substituents (CN, F,  $C_nF_{2n+1}$ ). Among heterocyclic molecules, hexaazatriphenylenes (HATs) and hexaazatrinaphthylenes (HATNAs) have shown remarkable charge carrier mobilities (up to  $0.9 \text{ cm}^2 \text{ V}^{-1} \text{ s}^{-1}$ ) along the columnar stacks in discotic liquid crystals as well as in amorphous materials (Chart 1).<sup>2</sup>

As an upper limit for the electron affinity a value of 4.0 eV has been suggested.<sup>1f</sup> Devices constructed from systems with higher  $EA$  will hardly be stable toward environmental reductants under ambient operation conditions. The inherent instability of

**Chart 1**

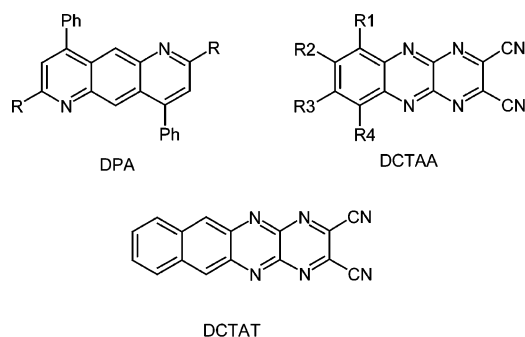


intermediate organic anions toward oxidation, on the other hand, is the main reason for the small number of studies on n-channel as compared to p-channel OTFTs.<sup>1d,f</sup> The problem of air stability has been addressed in terms of formal redox potentials by de Leeuw et al.<sup>3</sup> One efficient way to stabilize organic n-type materials is the introduction of fluorinated alkyl chains that probably prevent the diffusion of  $\text{H}_2\text{O}$  and  $\text{O}_2$  into the film and lead to kinetic stabilization.<sup>1d,f,4</sup> An alternative approach could be the design of materials in which the monomeric units form highly interconnected aggregates (e.g., hydrogen-bonded networks) with small interlayer spacing so that diffusion of small molecules into the channel is prevented, and trapping reactions of intermediate anions become energetically costly as the regular network structure is destroyed.

The second important quantity in eq 1 is the transfer integral  $t$  that depends on the relative arrangement of the molecules in the solid state and describes the intermolecular electronic coupling which needs to be maximized to achieve high charge carrier mobilities. This quantity has been approximated as half the splitting of the HOMO levels (hole transport) or LUMO

- (2) (a) Lemaire, V.; da Silva Filho, D. A.; Coropceanu, V.; Lehmann, M.; Geerts, Y.; Piris, J.; Debije, M. G.; van de Craats, A. M.; Senthikumar, K.; Siebbeles, L. D. A.; Warman, J. M.; Bredas, J.-L.; Cornil, G. *J. Am. Chem. Soc.* **2004**, *126*, 3271 and references given therein. (b) Kaafarani, B. R.; Kondo, T.; Yu, J.; Zhang, Q.; Dattilo, D.; Risko, C.; Jones, S. C.; Barlow, F.; Domercq, B.; Amy, F.; Kahn, A.; Bredas, J.-L.; Kippelen, B.; Marder, S. R. *J. Am. Chem. Soc.* **2005**, *127*, 16358 and references given therein.
- (3) de Leeuw, D. M.; Simenon, M. M. J.; Brown, A. R.; Einerhand, R. E. F. *Synth. Met.* **1997**, *87*, 53.
- (4) (a) Katz, H. E.; Johnson, J.; Lovinger, A. J.; Li, W. *J. Am. Chem. Soc.* **2000**, *122*, 7787. (b) Katz, H. E.; Lovinger, A. J.; Johnson, J.; Kloc, C.; Siegrist, T.; Li, W.; Lin, Y.-Y.; Dodabalapur, A. *Nature* **2000**, *404*, 478. Stabilization, presumably due to electronic effects, has also been reported for perylene bisimides upon introduction of cyano groups: (c) Jones, B. A.; Ahrens, M. J.; Yoon, M.-H.; Facchetti, A.; Marks, T. J.; Wasielewski, M. R. *Angew. Chem., Int. Ed.* **2004**, *43*, 6363.

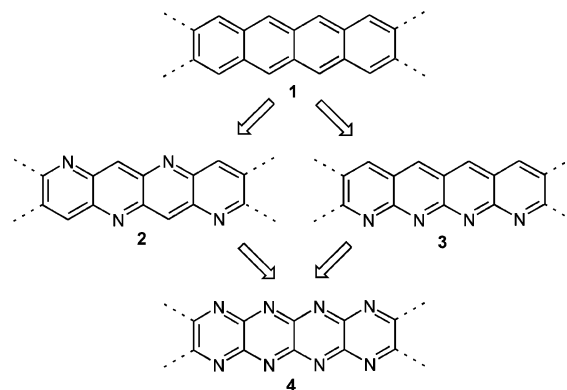
Chart 2



levels (electron transport) induced by interaction of two stacked molecules.<sup>1,5</sup> Recent experimental and computational results indicate that cofacial arrangements with high contact areas between the  $\pi$ -faces lead to particularly high charge carrier mobilities in both p-type and n-type semiconductors.<sup>1</sup> Most solid oligoacene phases adopt a herringbone structure that reflects a compromise between opposing intermolecular interactions (quadrupolar interactions that favor edge-to-face arrangements as in solid benzene versus dispersive interactions that favor face-to-face  $\pi$ -stacking).<sup>1,6</sup> Accordingly, the relative abundance of C–H versus C–C interactions determines the solid-state structure of polycyclic aromatic hydrocarbons (PAHs) where the preference for a herringbone structure decreases with a lower relative number of C–H contacts, and the structures become more graphite-like in hydrogen-poor systems.<sup>1,6</sup> Appropriate substitution in oligoacenes has been shown to have a similar effect, although crystal structures of substituted PAHs are difficult to predict a priori.

Whereas substituted oligoacenes have been the subject of many investigations,<sup>7</sup> few studies focused so far on heterocyclic derivatives.<sup>8</sup> The potential of nitrogen-containing oligoacenes as n-channel organic semiconductors has been demonstrated for diphenylanthrazolines (DPAs, Chart 2),<sup>8a</sup> dicyanotetraazaanthracenes (DCTAA), and dicyanotetraazaacene (DCTAT).<sup>8b</sup>

Scheme 1



Although the charge carrier mobilities for the latter systems are still rather low ( $10^{-6}$ – $10^{-8}$  cm<sup>2</sup> V<sup>-1</sup> s<sup>-1</sup> without optimization), the compounds clearly show n-channel field effect activity, and significantly higher mobilities can be expected for nitrogen-rich pentacenes or hexacenes.

In addition to strongly enhanced electron affinities, the successive replacement of CH moieties by nitrogen atoms in oligoacenes offers a number of opportunities to manipulate and control the molecular electronic properties, stabilities, and crystal structures of these materials. Thus, improved stability toward photooxidation or Diels–Alder dimerization (two major degradation pathways in pentacene semiconductors)<sup>1,9</sup> can be expected, and depending on the heteroatomic substitution pattern (polarity), improved solubility might be achieved as a basic prerequisite for solution-processing. A most interesting question is how substitution of CH by N modifies the solid-state structures (and hence the transfer integrals) of azaoligoacenes.

We have investigated representative compounds **2–4**, in which the number of nitrogens is equal to or twice the number of annellated benzene rings (Scheme 1). The focus is on structures and electronic properties of monomeric molecules. Oligomers of these systems, including a determination of transfer integrals for different intermolecular orientations, will be the subject of future work.

### Computational Methods

Geometries and vibrational frequencies of the singlet ground states of systems **1–4** as well as the lowest triplet states, radical cations, and radical anions were calculated at the B3LYP/6-31G(d) level of theory.<sup>10</sup> For single-point energies the more flexible valence-triple- $\zeta$  6-311+G-(d,p) basis set was employed.<sup>11</sup> Tight convergence criteria for gradients and a full (99, 590) integration grid were used throughout. The stability of singlet wavefunctions constructed from restricted Kohn–Sham orbitals was tested by calculating the eigenvalues of the Hermitian stability matrices **A** and **B**.<sup>12</sup> Only for hexacene a triplet instability exists, but breaking the spin-symmetry results in a very modest decrease in energy of less than 0.2 kcal mol<sup>-1</sup>. Thus, RDFT results for singlet states are discussed throughout. The length of the acenes is denoted

- (5) General overview: (a) Cornil, J.; Beljonne, D.; Calbert, J. P.; Bredas, J.-L. *Adv. Mater.* **2001**, *13*, 1053. Representative examples: (b) Deng, W. Q.; Goddard, W. A. *J. Phys. Chem. B* **2004**, *108*, 8614. (c) Hutchison, G. R.; Ratner, M. A.; Marks, T. J. *J. Am. Chem. Soc.* **2005**, *127*, 16866. (d) Raghunath, P.; Reddy, M. A.; Gouri, C.; Bhanuprakash, K.; Rao, V. J. *J. Phys. Chem. A* **2006**, *110*, 1152. For a critical approach to the estimation of transfer integrals, see: (d) Valeev, E. F.; Coropceanu, V.; da Silva, Filho, D. A.; Salman, S.; Bredas, J. L. *J. Am. Chem. Soc.* **2006**, *128*, 9882. (6) (a) Gavezotti, A.; Desiraju, G. R. *Acta Crystallogr., Sect. B* **1988**, *44*, 427. (b) Desiraju, G. R.; Gavezotti, A. *Acta Crystallogr., Sect. B* **1989**, *45*, 473. (7) For example: Chen, H. Y.; Chao, I. *Chem. Phys. Lett.* **2005**, *401*, 539. For experimental studies, see ref 9. (8) (a) Tonzola, C. J.; Alam, M. M.; Kaminsky, W.; Jenekhe, S. A. *J. Am. Chem. Soc.* **2003**, *125*, 13548. (b) Nishida, J.-I.; Naraso; Murai, S.; Fujiwara, E.; Tada, H.; Tomura, M.; Yamashita, Y. *Org. Lett.* **2004**, *6*, 2007. (c) Tadokoro, M.; Yasuzuka, S.; Nakamura, M.; Shinoda, T.; Tatenuma, T.; Mitsumi, M.; Qzawa, Y.; Toriumi, K.; Yoshino, H.; Shiomi, D.; Sato, K.; Takui, T.; Mori, T.; Murata, K. *Angew. Chem., Int. Ed.* **2006**, *45*, 5144. See also: (d) Hutchison, K. A.; Srdanov, G.; Hicks, R.; Yu, H.; Wudl, F.; Strassner, T.; Nendel, M.; Houk, K. N. *J. Am. Chem. Soc.* **1998**, *120*, 2989. (e) Wudl, F.; Koutentis, P. A.; Weiz, A.; Ma, B.; Strassner, T.; Houk, K. N.; Khan, S. I. *Pure Appl. Chem.* **1999**, *71*, 295. (f) Riley, A. E.; Mitchell, G. W.; Koutentis, P. A.; Bendikov, M.; Kaszynski, P.; Wudl, F.; Tolbert, S. H. *Adv. Funct. Mater.* **2003**, *13*, 531. (g) Constantinides, C. P.; Koutentis, P. A.; Schatz, J. *J. Am. Chem. Soc.* **2004**, *126*, 16232. (h) Langer, P.; Bodtke, A.; Saleh, N. N. R.; Görls, H.; Schreiner, P. R. *Angew. Chem., Int. Ed.* **2005**, *44*, 5255. Aza-hydroacenes have shown remarkable hole mobilities in amorphous films. For detailed studies, see: (i) Miao, Q.; Nguyen, T.-Q.; Someya, T.; Blanchet, G. B.; Nuckolls, C. J. *J. Am. Chem. Soc.* **2003**, *125*, 10284. (j) Ma, Y.; Sun, Y.; Liu, Y.; Gao, J.; Chen, S.; Sun, X.; Qiu, W.; Yu, G.; Cui, G.; Hu, W.; Zhu, D. *J. Mater. Chem.* **2005**, *15*, 4894. Very recently, some of the pentacenes discussed in this work have been studied computationally under similar aspects by Chao et al.: (k) Chen, H.-Y.; Chao, I. *Chem. Phys. Chem.* **2006**, *7*, 2003.

- (9) For example, see: (a) Payne, M. M.; Odom, S. A.; Parkin, S. R.; Anthony, J. E. *Org. Lett.* **2004**, *6*, 3325. (b) Maliakal, A.; Raghavachari, K.; Katz, H.; Chandross, E.; Siegrist, T. *Chem. Mater.* **2004**, *16*, 4980. (c) Payne, M. M.; Parkin, S. R.; Anthony, J. E.; Kuo, C.; Jackson, T. N. *J. Am. Chem. Soc.* **2005**, *127*, 8028. (d) Chien, S.-H.; Cheng, M.-F.; Lau, K. C.; Li, W. K. *J. Phys. Chem. A* **2005**, *109*, 7509. (10) (a) Hehre, W. J.; Ditchfield, R.; Pople, J. A. *J. Chem. Phys.* **1972**, *56*, 2257. (b) Lee, C.; Yang, W.; Parr, R. G. *Phys. Rev. B* **1988**, *37*, 785. (c) Becke, A. D. *J. Chem. Phys.* **1993**, *98*, 5648. (11) Krishnan, R.; Binkley, J. S.; Seeger, R.; Pople, J. A. *J. Chem. Phys.* **1980**, *72*, 650. (12) Bauernschmitt, R.; Ahlrichs, R. *J. Chem. Phys.* **1996**, *104*, 9047.

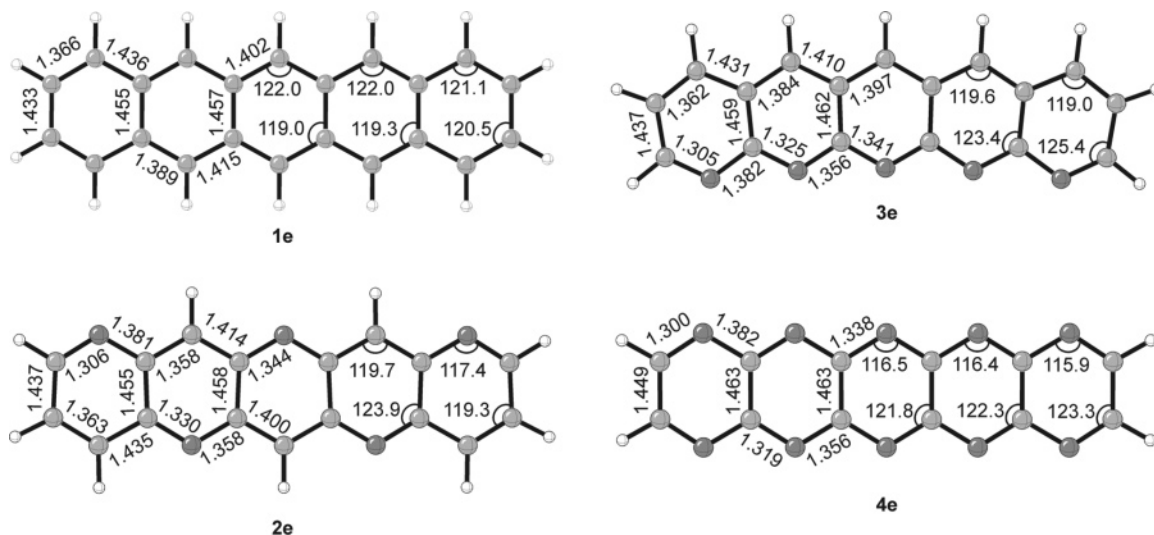


**Figure 2.** Selected structural parameters (bond lengths in Å, angles in deg) of pentacene **1e** and its aza derivatives **2e**–**4e**.

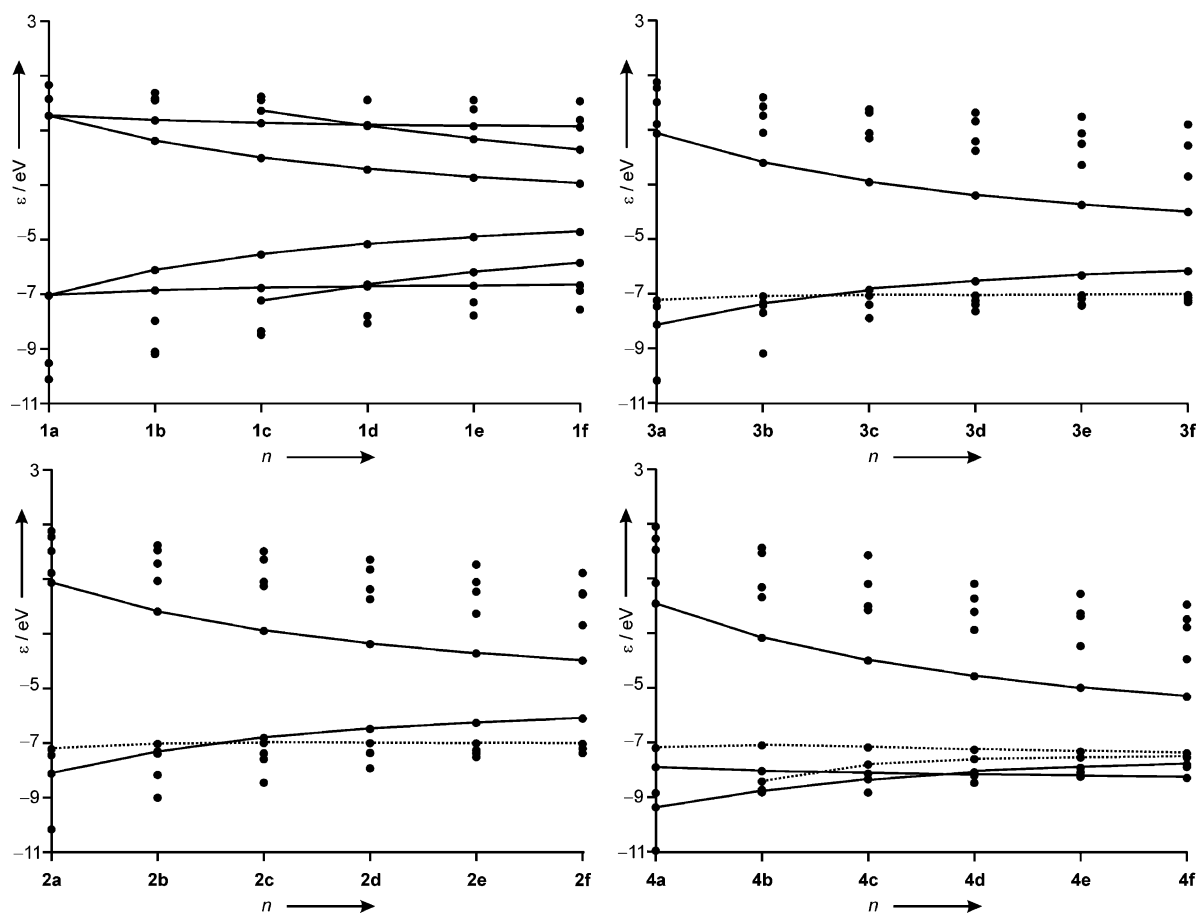


**Figure 3.** Energies of frontier molecular orbitals of **1a**–**f**, **2a**–**f**, **3a**–**f**, and **4a**–**f**, as a function of acene length. Solid lines refer to π-orbitals; dotted lines indicate σ orbitals.

by a letter following the compound number (a, b, c, ... for systems of 1, 2, 3, ... annelated rings). Thus, **2d** refers to a tetraazatetracene, **4e**, to a decaazapentacene, etc. If not mentioned otherwise, all energies discussed in the text refer to electronic energies obtained at the 6-311+G(d,p)//6-31G(d) level. Zero-point vibrational energy corrections (ZPVE) are given in the Supporting Information. All calculations were carried out with Gaussian98<sup>13a</sup> and Gaussian03.<sup>13b</sup>

(13) (a) Frisch, M. J. et al. *Gaussian 98*; Gaussian, Inc.: Pittsburgh, PA, 1998.  
(b) Frisch, M. J. et al. *Gaussian 03*; Gaussian, Inc.: Pittsburgh, PA, 2003.

## Results and Discussion

Pentacenes are probably the most promising candidates for prospective device applications and will be discussed in some detail, whereas the smaller and larger homologues are treated in comparison to them. The optimized geometries of **1e**–**4e** are shown in Figure 2. All structures are planar and highly symmetric ( $D_{2h}$  for **1** and **4**;  $C_{2v}$  for **3**, **2a**, **2c**, and **2e**;  $C_{2h}$  for **2b**, **2d**, and **2f**), although the lowest frequency out-of-plane

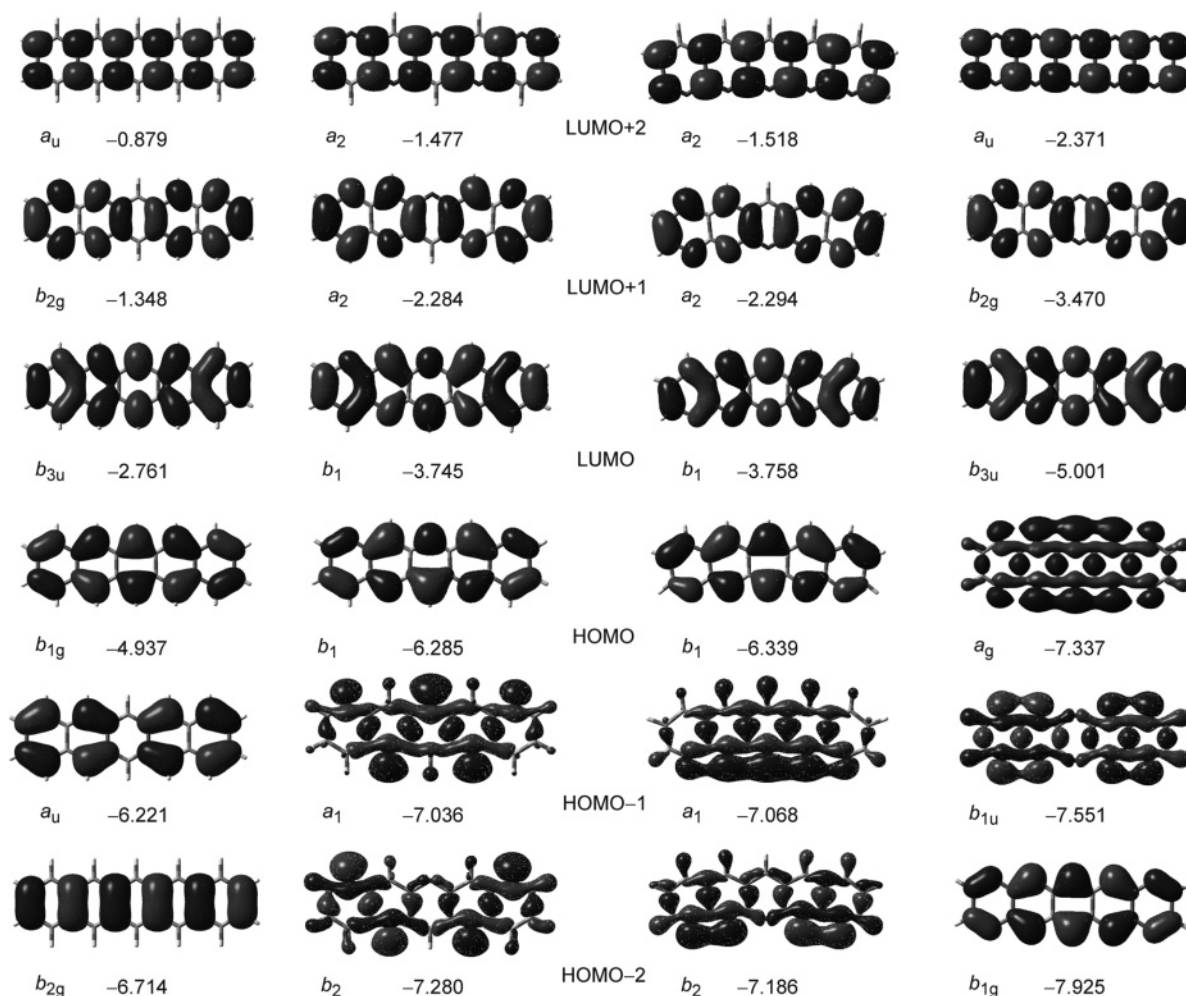


**Figure 4.** Highest occupied and lowest unoccupied molecular orbitals of **1e–4e**. Orbital energies are given in eV.

vibrational mode is in the range of only  $30\text{ cm}^{-1}$  for the hexacenes, indicating increasing molecular flexibility with increasing length of the molecules. The C–N bonds are generally shorter than the C–C bonds, and the CNC angles are slightly below  $120^\circ$  to maximize the  $s$  character of the lone-pair orbitals, so that **3** adopts a curved shape. The annellated pyridines show a strong dipole moment that increases from 2.37 D in pyridine **3a** to 12.82 D in hexaazahexacene **3f**. Considering the longer acenes as two interacting polyacetylene chains,<sup>14</sup> the intrachain bond length alternation is significant in the terminal rings and decreases toward the center of the molecule. The interchain bonds approach a length of approximately  $1.46\text{ \AA}$  in all four series.

To clarify tendencies in electronic properties, the energies  $\epsilon$  of the five highest occupied and lowest unoccupied molecular orbitals (HOMOs and LUMOs) are given as a function of the number of annellated rings  $n$  in Figure 3. The orbitals for pentacenes **1e–4e** are depicted graphically in Figure 4. The HOMO–LUMO gaps in all four series decrease with increasing acene length and converge toward a constant value that is almost reached for  $n = 6$  (Table 1). Basis set enlargement from 6-31G-(d) to 6-311+G(d,p) consistently lowers all HOMO energies by  $0.3\text{--}0.4\text{ eV}$  and the LUMO energies by  $0.3\text{--}0.5\text{ eV}$ , so that

the overall HOMO–LUMO gaps are largely independent of the basis set size. Most importantly, the symmetry of the HOMOs is different in the four series of compounds. The energy of the  $\pi$  orbitals goes down with an increasing number of electronegative nitrogen atoms in the molecule. In the entire pyrazinopyrazine series **4** the HOMO is the totally symmetric linear combination of the nitrogen lone pairs, i.e., a  $\sigma$  orbital; the higher energy of the  $a_g$  symmetric combination of the lone pair orbitals in pyrazine **4a** compared to the out-of-phase  $b_{1u}$  orbital is a classic example of through-bond interaction and has been studied in some detail.<sup>15</sup> In **2** and **3** the nature of the HOMO changes with increasing length of the acene. In **2a/2b** and **3a/3b** the  $\sigma$ -orbital is higher in energy than the highest  $\pi$  MO, and in **2c** and **3c** the highest occupied  $\sigma$ - and  $\pi$ -orbitals are almost degenerate, whereas the latter become the HOMO in the larger pyridinopyridines. The overall HOMO–LUMO gaps of aza-pentacenes and hexacenes are larger than those for **1e** and **1f**, indicating a more pronounced stabilization of the HOMO compared to the LUMO upon introduction of nitrogen atoms.

Although Koopmans' theorem is not strictly valid in density functional theory,<sup>16</sup> the calculated vertical ionization potentials ( $IE_{\text{vert}}$ ) reflect the tendencies in Kohn–Sham orbital energies (Figure 5, Table 2). The absolute values, however, are signifi-

(14) (a) Houk, K. N.; Lee, P. S.; Nendel, M. *J. Org. Chem.* **2001**, *66*, 5517. (b) Bendikov, M.; Duong, H. M.; Starkey, K.; Houk, K. N.; Carter, E. A.; Wudl, F. *J. Am. Chem. Soc.* **2004**, *126*, 7416; correction: 10493.

(15) Gleiter, R. *Angew. Chem., Int. Ed. Engl.* **1974**, *13*, 696.

(16) Koch, W.; Holthausen, M. C. *A Chemist's Guide to Density Functional Theory*; Wiley-VCH: Weinheim, 2000 and references given therein.

**Table 1.** Energies of Frontier Molecular Orbitals and HOMO–LUMO Gaps (in eV) of Acenes **1** and Azaacenes **2–4**<sup>a</sup>

|                          | a               | b               | c               | d               | e               | f               |
|--------------------------|-----------------|-----------------|-----------------|-----------------|-----------------|-----------------|
| <b>1</b>                 |                 |                 |                 |                 |                 |                 |
| $\epsilon_{\text{HOMO}}$ | -7.074 (-6.702) | -6.143 (-5.788) | -5.574 (-5.225) | -5.199 (-4.856) | -4.937 (-4.598) | -4.746 (-4.411) |
| $\epsilon_{\text{LUMO}}$ | -0.490 (+0.099) | -1.412 (-0.959) | -2.039 (-1.632) | -2.462 (-2.077) | -2.761 (-2.387) | -2.979 (-2.613) |
| $\Delta\epsilon$         | 6.584 (6.603)   | 4.731 (4.829)   | 3.535 (3.593)   | 2.737 (2.779)   | 2.176 (2.211)   | 1.767 (1.798)   |
| <b>2</b>                 |                 |                 |                 |                 |                 |                 |
| $\epsilon_{\text{HOMO}}$ | -7.247 (-6.873) | -7.055 (-6.665) | -6.832 (-6.483) | -6.507 (-6.158) | -6.285 (-5.936) | -6.127 (-5.778) |
| $\epsilon_{\text{LUMO}}$ | -1.151 (-0.611) | -2.211 (-1.767) | -2.916 (-2.508) | -3.398 (-3.006) | -3.745 (-3.360) | -4.004 (-3.624) |
| $\Delta\epsilon$         | 6.096 (6.262)   | 4.844 (4.898)   | 3.916 (3.975)   | 3.109 (3.152)   | 2.540 (2.576)   | 2.123 (2.154)   |
| <b>3</b>                 |                 |                 |                 |                 |                 |                 |
| $\epsilon_{\text{HOMO}}$ | -7.247 (-6.873) | -7.103 (-6.730) | -6.867 (-6.521) | -6.554 (-6.210) | -6.339 (-5.996) | -6.186 (-5.844) |
| $\epsilon_{\text{LUMO}}$ | -1.151 (-0.611) | -2.218 (-1.776) | -2.926 (-2.521) | -3.411 (-3.023) | -3.758 (-3.381) | -4.017 (-3.646) |
| $\Delta\epsilon$         | 6.096 (6.262)   | 4.885 (4.954)   | 3.941 (4.000)   | 3.143 (3.187)   | 2.581 (2.615)   | 2.169 (2.198)   |
| <b>4</b>                 |                 |                 |                 |                 |                 |                 |
| $\epsilon_{\text{HOMO}}$ | -7.201 (-6.832) | -7.105 (-6.714) | -7.182 (-6.783) | -7.266 (-6.864) | -7.337 (-6.934) | -7.395 (-6.991) |
| $\epsilon_{\text{LUMO}}$ | -1.914 (-1.421) | -3.172 (-2.740) | -4.001 (-3.595) | -4.578 (-4.184) | -5.001 (-4.614) | -5.324 (-4.941) |
| $\Delta\epsilon$         | 5.287 (5.411)   | 3.933 (3.974)   | 3.181 (3.188)   | 2.688 (2.680)   | 2.336 (2.320)   | 2.071 (2.050)   |

<sup>a</sup> B3LYP/6-31G(d) values are given in parentheses.

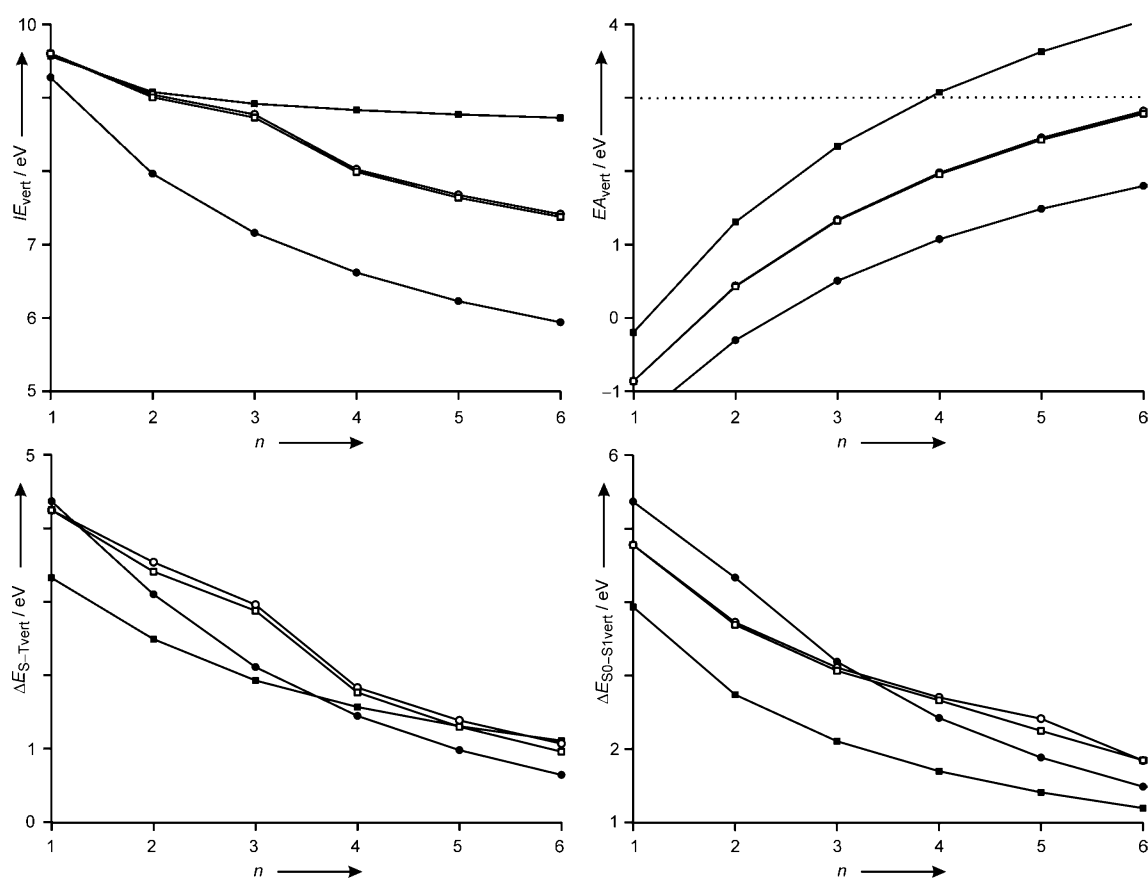


**Figure 5.** Vertical ionization energies, electron affinities, singlet–triplet energy splittings, and energies of the first excited singlet states of acenes and azaacenes (**1**, black circles; **2**, white squares; **3**, white circles; **4**, black squares).

cantly higher than expected from one-electron considerations. The  $IE$ s of acenes decrease monotonically from **1a** to **1f**. With the exception of **1a**, the calculated values are smaller than the best experimental data by 0.2–0.4 eV.<sup>17</sup> With the less flexible 6-31G(d) basis set, the underestimation is more significant by another 0.3 eV. The vertical  $IE$ s of **4** are considerably higher than that of **1** and decrease only modestly with the size of the

molecule. Very similar ionization energies are calculated for **2** and **3**. The radical cations of the first members of both series (**2a**, **2b**, **3a**, and **3b**) possess  $\sigma$  ground states, whereas the ground states of the higher pyridinopyridines **2d–2f** and **3d–3f** are of  $\pi$  symmetry, as expected on the basis of Koopmans' theorem. The  $IE$ s of the latter systems are approximately 1.5 eV higher than that of the parent hydrocarbons, whereas for the former  $IE$ s very similar to the corresponding pyrazines are obtained. For the radical cations of anthracenes **2c** and **3c** the lowest energy  $\sigma$  and  $\pi$  electronic states are close in energy, and the ordering depends strongly on basis set and geometry.<sup>18</sup>

(17) Experimental ionization potentials for **1a–1f** are 9.24, 8.14, 7.44, 6.97, 6.63, and 6.4 eV. Very similar  $IE$ s are found for pyridine (9.26 eV) and pyrazine (9.28 eV): (a) *NIST Chemistry Webbook*, <http://webbook.nist.gov>. See also: (b) Deleuze, M. S.; Claes, L.; Kryachko, E. S.; Francois, J.-P. *J. Chem. Phys.* **2003**, *119*, 3106.

**Table 2.** Vertical and Adiabatic Ionization Energies and Electron Affinities (in eV) of Acenes **1** and Azaacenes **2–4**<sup>a</sup>

|                    | a               | b               | c             | d             | e             | f             |
|--------------------|-----------------|-----------------|---------------|---------------|---------------|---------------|
|                    | <b>1</b>        |                 |               |               |               |               |
| $IE_{\text{vert}}$ | 9.275 (9.011)   | 7.964 (7.688)   | 7.159 (6.873) | 6.618 (6.326) | 6.229 (5.935) | 5.939 (5.643) |
| $IE_{\text{adia}}$ | 9.132 (8.858)   | 7.877 (7.595)   | 7.094 (6.804) | 6.565 (6.270) | 6.185 (5.888) | 5.901 (5.603) |
| $EA_{\text{vert}}$ | -1.435 (-2.306) | -0.305 (-0.898) | 0.505 (0.006) | 1.073 (0.618) | 1.486 (1.056) | 1.798 (1.384) |
| $EA_{\text{adia}}$ | -1.294 (-2.103) | -0.200 (-0.766) | 0.589 (0.107) | 1.140 (0.699) | 1.540 (1.123) | 1.841 (1.440) |
|                    | <b>2</b>        |                 |               |               |               |               |
| $IE_{\text{vert}}$ | 9.602 (9.368)   | 9.006 (8.726)   | 8.729 (8.422) | 7.989 (7.699) | 7.638 (7.340) | 7.377 (7.074) |
| $IE_{\text{adia}}$ | 9.117 (8.883)   | 8.628 (8.354)   | 8.407 (8.117) | 7.926 (7.629) | 7.586 (7.282) | 7.333 (7.026) |
| $EA_{\text{vert}}$ | -0.863 (-1.680) | 0.429 (-0.163)  | 1.326 (0.816) | 1.959 (1.488) | 2.426 (1.977) | 2.782 (2.348) |
| $EA_{\text{adia}}$ | -0.720 (-1.455) | 0.542 (-0.021)  | 1.417 (0.926) | 2.036 (1.578) | 2.491 (2.054) | 2.839 (2.415) |
|                    | <b>3</b>        |                 |               |               |               |               |
| $IE_{\text{vert}}$ | 9.602 (9.368)   | 9.041 (8.769)   | 8.771 (8.480) | 8.024 (7.740) | 7.675 (7.384) | 7.413 (7.117) |
| $IE_{\text{adia}}$ | 9.117 (8.883)   | 8.752 (8.490)   | 8.439 (8.154) | 7.963 (7.670) | 7.621 (7.321) | 7.362 (7.057) |
| $EA_{\text{vert}}$ | -0.863 (-1.680) | 0.434 (-0.155)  | 1.337 (0.832) | 1.977 (1.512) | 2.451 (2.010) | 2.817 (2.392) |
| $EA_{\text{adia}}$ | -0.720 (-1.455) | 0.549 (-0.013)  | 1.432 (0.943) | 2.057 (1.606) | 2.523 (2.093) | 2.884 (2.470) |
|                    | <b>4</b>        |                 |               |               |               |               |
| $IE_{\text{vert}}$ | 9.564 (9.325)   | 9.076 (8.794)   | 8.917 (8.612) | 8.831 (8.510) | 8.771 (8.439) | 8.725 (8.385) |
| $IE_{\text{adia}}$ | 9.185 (8.961)   | 8.761 (8.500)   | 8.659 (8.377) | 8.612 (8.316) | 8.578 (8.273) | 8.547 (8.238) |
| $EA_{\text{vert}}$ | -0.199 (-0.966) | 1.307 (0.718)   | 2.338 (1.820) | 3.074 (2.592) | 3.625 (3.164) | 4.052 (3.605) |
| $EA_{\text{adia}}$ | -0.033 (-0.704) | 1.443 (0.887)   | 2.454 (1.955) | 3.174 (2.708) | 3.714 (3.267) | 4.135 (3.700) |

<sup>a</sup> B3LYP/6-31G(d) values are given in parentheses.**Table 3.** Singlet–Triplet Energy Splittings and Energies of the Lowest Excited Singlet States (in eV) of Acenes **1** and Azaacenes **2–4**<sup>a</sup>

|                                | a             | b             | c             | d             | e             | f             |
|--------------------------------|---------------|---------------|---------------|---------------|---------------|---------------|
|                                | <b>1</b>      |               |               |               |               |               |
| $\Delta E_{\text{ST,vert}}$    | 4.377 (4.446) | 3.108 (3.148) | 2.118 (2.136) | 1.452 (1.463) | 0.986 (0.994) | 0.649 (0.656) |
| $\Delta E_{\text{ST,adia}}$    | 3.846 (3.882) | 2.700 (2.717) | 1.808 (1.812) | 1.202 (1.201) | 0.778 (0.775) | 0.471 (0.469) |
| $\Delta E_{\text{S0-S1,vert}}$ | 5.376 (5.548) | 4.339 (4.461) | 3.194 (3.276) | 2.428 (2.493) | 1.889 (1.944) | 1.492 (1.542) |
|                                | <b>2</b>      |               |               |               |               |               |
| $\Delta E_{\text{ST,vert}}$    | 4.257 (4.361) | 3.419 (3.506) | 2.885 (2.902) | 1.772 (1.792) | 1.304 (1.320) | 0.964 (0.977) |
| $\Delta E_{\text{ST,adia}}$    | 3.639 (3.717) | 2.921 (2.949) | 2.462 (2.462) | 1.476 (1.482) | 1.052 (1.058) | 0.745 (0.750) |
| $\Delta E_{\text{S0-S1,vert}}$ | 4.786 (4.913) | 3.698 (3.733) | 3.071 (3.071) | 2.669 (2.653) | 2.252 (2.308) | 1.851 (1.901) |
|                                | <b>3</b>      |               |               |               |               |               |
| $\Delta E_{\text{ST,vert}}$    | 4.257 (4.361) | 3.547 (3.588) | 2.967 (2.991) | 1.838 (1.856) | 1.392 (1.403) | 1.074 (1.081) |
| $\Delta E_{\text{ST,adia}}$    | 3.639 (3.717) | 2.991 (3.016) | 2.547 (2.527) | 1.552 (1.553) | 1.150 (1.146) | 0.865 (0.859) |
| $\Delta E_{\text{S0-S1,vert}}$ | 4.786 (4.913) | 3.732 (3.779) | 3.115 (3.129) | 2.709 (2.708) | 2.417 (2.409) | 1.848 (1.898) |
|                                | <b>4</b>      |               |               |               |               |               |
| $\Delta E_{\text{ST,vert}}$    | 3.334 (3.410) | 2.498 (2.510) | 1.936 (1.917) | 1.574 (1.543) | 1.313 (1.276) | 1.116 (1.078) |
| $\Delta E_{\text{ST,adia}}$    | 3.238 (3.319) | 2.086 (2.109) | 1.557 (1.554) | 1.201 (1.188) | 0.948 (0.933) | 0.746 (0.732) |
| $\Delta E_{\text{S0-S1,vert}}$ | 3.941 (4.037) | 2.747 (2.767) | 2.110 (2.099) | 1.702 (1.677) | 1.414 (1.383) | 1.199 (1.165) |

<sup>a</sup> B3LYP/6-31G(d) values are given in parentheses.

The singlet–triplet energy splittings  $\Delta E_{\text{S-T}}$  of the acenes **1** and **4** decrease monotonically with  $n$  (Table 3).<sup>14</sup> The pyrazinopyrazines **4** converge toward a higher  $\Delta E_{\text{S-T}}$  and all azaacenes with  $n \geq 4$  have larger singlet–triplet splittings than the hydrocarbons, as expected from the higher HOMO–LUMO gaps. The  $\Delta E_{\text{S-T}}$  vs  $n$  behavior for pyridinopyridines **2a–2c** and **3a–3c** parallels that of **4**, whereas the tendencies for **2d–2f** and **3d–3f** are parallel to those for **1**. The lowest triplet state in the former systems is of  $\sigma-\pi$  type (i.e., one unpaired electron occupies a  $\sigma$  orbital, and the other one, a  $\pi$  orbital), and in the latter the singly occupied MOs are both of  $\pi$  symmetry. Analogous to the radical cations, the triplet states of **2c** and **3c** are characterized by electronic near-degeneracies, and the symmetry of the lowest triplet state depends sensitively on the structure and level of theory. For a given state, on the other hand, the singlet–triplet splitting is largely independent of the

basis set flexibility, and almost identical values are obtained with the double- and triple- $\zeta$  sets for all compounds.

The vertical excitation energies to the S1 state as obtained from time-dependent DFT calculations also decrease with increasing length of the acene. The pyrazinopyrazines **4** have significantly lower excitation energies than the corresponding oligoacenes **1**, whereas  $\Delta E_{\text{S0-S1}}$  of the pyridinopyridines **2** and **3** is slightly larger than that of **1** for  $n \geq 4$ . For the hydrocarbons, the calculated excitation energies agree reasonably with available experimental values.<sup>14,19</sup>

The electron affinities ( $EA$ ) of all four series increase monotonically with the size of the systems. Not surprisingly, the 6-31G(d) basis set is not flexible enough to describe the anion states correctly and significantly underestimates the  $EA$  of all compounds by 0.4–0.7 eV, whereas good agreement with experiment is achieved at the 6-311+G(d,p)//6-31G(d) level.<sup>20</sup>

(18) For consistency the  ${}^2A_1$  states of **2c**<sup>+</sup> and **3c**<sup>+</sup> are considered in the text, although the vertical  $IE$  to the  ${}^2B_1$  state is lower by 0.244 and 0.260 eV, respectively. Convergence to the excited states is readily achieved by switching the occupancies of initial guess orbitals appropriately.

(19) Experimental excitation energies for **1a–1f** are 4.84, 3.97, 3.35, 2.61, 2.14, and 1.79 eV: (a) Birk, J. B. *Photophysics of Aromatic Molecules*; Wiley: New York, 1970. (b) Angliker, H.; Rommel, E.; Wirz, J. *Chem. Phys. Lett.* **1982**, *87*, 208.

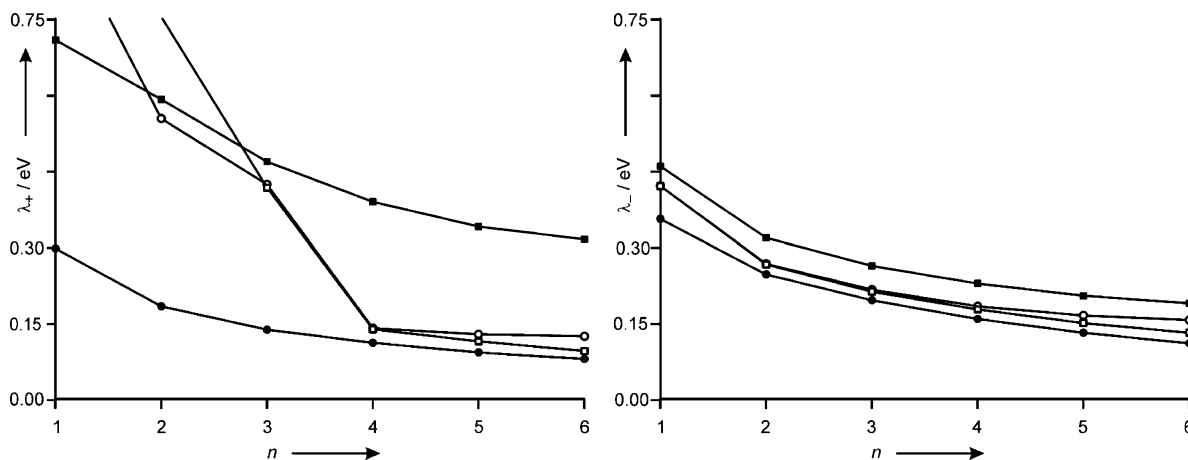


**Figure 6.** Reorganization energies of acenes and azaacenes. (1, black circles; 2, white squares; 3, white circles; 4, black squares). Note that  $\lambda_+$  is physically not particularly meaningful for systems as **2c** and **3c** where two near-degenerate states of the radical cations are involved, so that simple Marcus theory does not apply.

**Table 4.** Reorganization Energies (in eV) of Acenes **1** and Azaacenes **2–4**<sup>a</sup>

|             | a             | b             | c             | d             | e             | f             |
|-------------|---------------|---------------|---------------|---------------|---------------|---------------|
| <b>1</b>    |               |               |               |               |               |               |
| $\lambda_1$ | 0.154 (0.150) | 0.096 (0.093) | 0.072 (0.069) | 0.058 (0.055) | 0.048 (0.046) | 0.041 (0.039) |
| $\lambda_2$ | 0.143 (0.153) | 0.087 (0.093) | 0.065 (0.069) | 0.053 (0.056) | 0.044 (0.047) | 0.038 (0.040) |
| $\lambda_3$ | 0.214 (0.203) | 0.141 (0.129) | 0.111 (0.099) | 0.091 (0.079) | 0.077 (0.065) | 0.067 (0.054) |
| $\lambda_4$ | 0.141 (0.203) | 0.105 (0.132) | 0.084 (0.101) | 0.067 (0.081) | 0.054 (0.067) | 0.043 (0.056) |
| $\lambda_+$ | 0.297 (0.303) | 0.183 (0.186) | 0.137 (0.138) | 0.111 (0.111) | 0.092 (0.093) | 0.079 (0.079) |
| $\lambda_-$ | 0.355 (0.406) | 0.246 (0.261) | 0.195 (0.200) | 0.158 (0.160) | 0.131 (0.132) | 0.110 (0.110) |
| <b>2</b>    |               |               |               |               |               |               |
| $\lambda_1$ | 0.471 (0.487) | 0.376 (0.401) | 0.095 (0.087) | 0.075 (0.069) | 0.062 (0.057) | 0.051 (0.047) |
| $\lambda_2$ | 0.485 (0.485) | 0.378 (0.372) | 0.322 (0.305) | 0.063 (0.070) | 0.052 (0.058) | 0.044 (0.048) |
| $\lambda_3$ | 0.277 (0.260) | 0.153 (0.140) | 0.121 (0.107) | 0.100 (0.088) | 0.085 (0.074) | 0.074 (0.064) |
| $\lambda_4$ | 0.143 (0.225) | 0.113 (0.142) | 0.091 (0.110) | 0.077 (0.090) | 0.065 (0.077) | 0.057 (0.067) |
| $\lambda_+$ | 0.956 (0.972) | 0.754 (0.773) | 0.417 (0.392) | 0.138 (0.139) | 0.114 (0.115) | 0.095 (0.095) |
| $\lambda_-$ | 0.420 (0.485) | 0.266 (0.282) | 0.212 (0.217) | 0.177 (0.178) | 0.150 (0.151) | 0.131 (0.131) |
| <b>3</b>    |               |               |               |               |               |               |
| $\lambda_1$ | 0.471 (0.487) | 0.264 (0.286) | 0.091 (0.083) | 0.079 (0.071) | 0.074 (0.065) | 0.073 (0.063) |
| $\lambda_2$ | 0.485 (0.485) | 0.289 (0.279) | 0.332 (0.326) | 0.061 (0.070) | 0.054 (0.063) | 0.051 (0.060) |
| $\lambda_3$ | 0.277 (0.260) | 0.152 (0.139) | 0.121 (0.109) | 0.103 (0.092) | 0.093 (0.082) | 0.089 (0.077) |
| $\lambda_4$ | 0.143 (0.225) | 0.115 (0.142) | 0.095 (0.111) | 0.080 (0.094) | 0.072 (0.083) | 0.067 (0.078) |
| $\lambda_+$ | 0.956 (0.972) | 0.553 (0.565) | 0.423 (0.409) | 0.140 (0.141) | 0.128 (0.128) | 0.124 (0.123) |
| $\lambda_-$ | 0.420 (0.485) | 0.267 (0.281) | 0.216 (0.220) | 0.183 (0.186) | 0.165 (0.165) | 0.156 (0.155) |
| <b>4</b>    |               |               |               |               |               |               |
| $\lambda_1$ | 0.329 (0.353) | 0.276 (0.316) | 0.210 (0.253) | 0.170 (0.214) | 0.147 (0.190) | 0.137 (0.181) |
| $\lambda_2$ | 0.379 (0.364) | 0.315 (0.294) | 0.258 (0.235) | 0.219 (0.194) | 0.193 (0.166) | 0.178 (0.147) |
| $\lambda_3$ | 0.293 (0.266) | 0.182 (0.164) | 0.147 (0.131) | 0.128 (0.112) | 0.115 (0.100) | 0.106 (0.092) |
| $\lambda_4$ | 0.166 (0.262) | 0.136 (0.169) | 0.116 (0.135) | 0.100 (0.116) | 0.089 (0.103) | 0.083 (0.095) |
| $\lambda_+$ | 0.708 (0.717) | 0.591 (0.610) | 0.468 (0.488) | 0.389 (0.408) | 0.340 (0.356) | 0.315 (0.328) |
| $\lambda_-$ | 0.459 (0.528) | 0.318 (0.333) | 0.263 (0.266) | 0.228 (0.228) | 0.204 (0.203) | 0.189 (0.187) |

<sup>a</sup> B3LYP/6-31G(d) values are given in parentheses.

To reach the desired high EA of 3 eV at least hexacenes are required in the pyridine series **2** and **3**, whereas this value is already reached with octaazatetracene **4d** in the pyrazinopyrazine series. From Figure 5 it can also be concluded that at least seven to eight nitrogens have to be incorporated into pentacene to make it a potentially useful n-channel semiconductor without adding additional electron-withdrawing substituents.

Reorganization energies for electron and hole transport of acenes and azaacenes are summarized in Figure 6 and Table 4.

(20) The most reliable experimental electron affinities for **1a–1e** are  $-1.12$ ,  $-0.20$ ,  $0.53$ ,  $1.07$ , and  $1.39$  eV, ref 15a. The EA reported for pyridine is still negative ( $-0.59$  eV), while that of pyrazine ( $-0.01$  eV) is close to zero. For a careful discussion, e.g., see: (a) Song, J. K.; Lee, N. K.; Kim, S. K. *J. Chem. Phys.* **2002**, *117*, 1589 and references given therein. The accuracy of DFT methods for the computation of EAs has been evaluated: (b) Rienstra-Kiracofe, J. C.; Tschumper, G.; Schaefer, H. F., III; Nandi, S.; Ellison, G. B. *Chem. Rev.* **2002**, *102*, 231.

In all systems  $\lambda_+$  and  $\lambda_-$  decrease with increasing length of the acenes and the hydrocarbons require the smallest reorganization energies. The calculated reorganization energies  $\lambda_+$  of **1** agree nicely with previous calculations<sup>1,5b</sup> as well as with experimental estimates.<sup>21</sup> Interestingly, a more flexible basis set increases the components  $\lambda_1/\lambda_3$  and decreases  $\lambda_2/\lambda_4$  to a comparable degree, so that the overall value for  $\lambda_+/\lambda_-$  is rather independent of the basis set employed.<sup>22</sup> The largest reorganization energies  $\lambda_+$  are obtained for those azaacenes in which ionization occurs from a  $\sigma$  orbital. The differences between the four series of compounds are less pronounced regarding the reorganization energies for

(21) Experimental reorganization energies reported for acenes **1c–1e** are 0.139, 0.118, and 0.099 eV, c.f. (a) Podzorov, V.; Sysoev, S. E.; Loginova, E.; Pudalov, V. M.; Gershenson, M. E. *Appl. Phys. Lett.* **2003**, *83*, 3504. (b) Podzorov, V.; Pudalov, V. M.; Gershenson, M. E. *Appl. Phys. Lett.* **2003**, *82*, 1739.

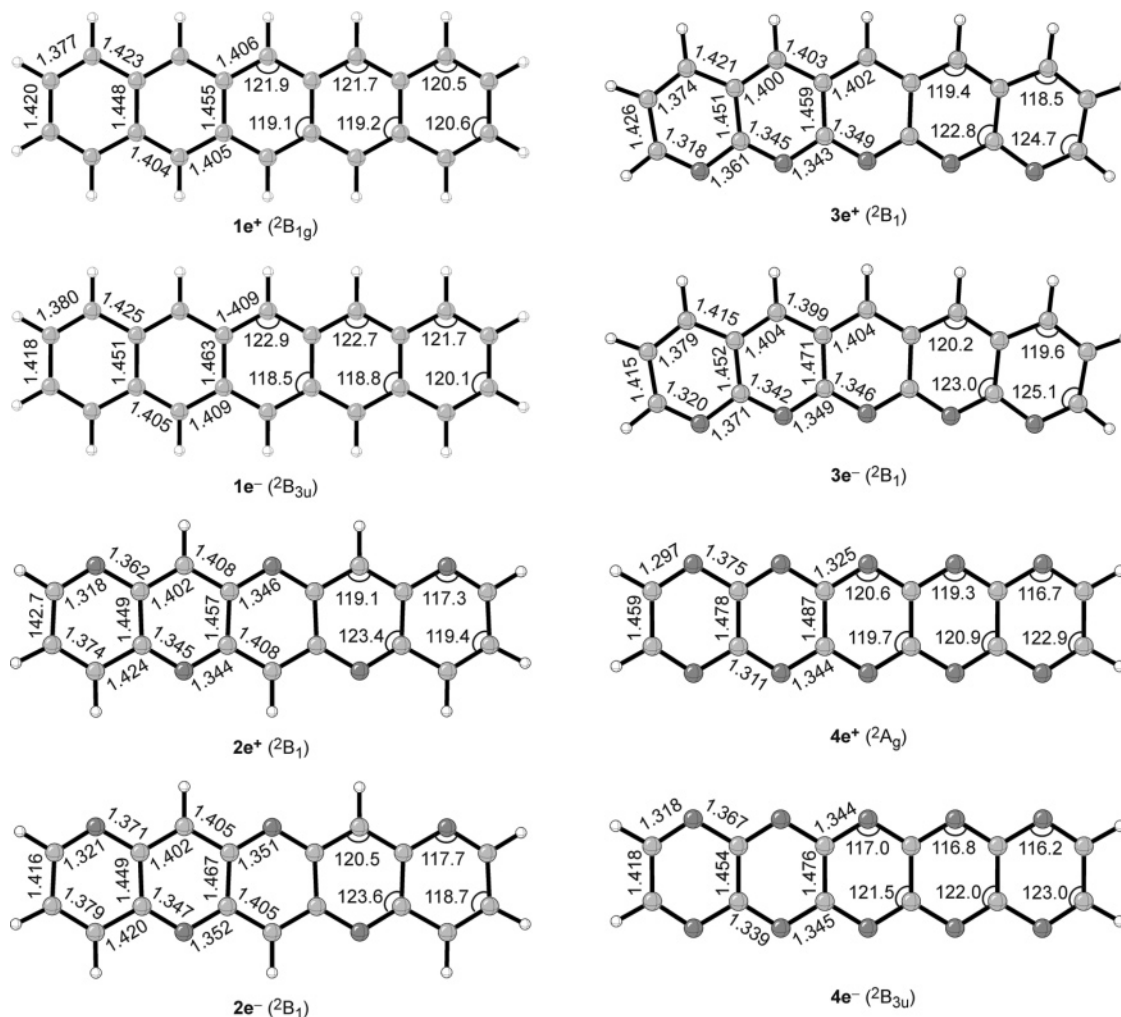
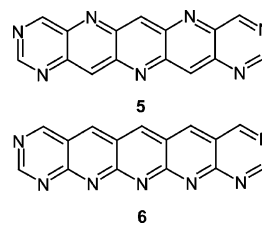


**Figure 7.** Selected structural parameters (bond lengths in Å, angles in deg) of pentacene radical cations and radical anions.

electron transfer  $\lambda_-$  that are more interesting in the present context. The pyrazinopyrazines **4** require reorganization energies that are 0.07–0.08 eV higher than that of oligoacenes **1**. The pyridinopyridines **2** and **3** require intermediate reorganization energies that are slightly lower for the former, especially for the pentacenes and hexacenes. These tendencies are partly reflected in the structural changes upon ionization or capture of an electron. The geometries of pentacene radical cations and radical anions are given in Figure 7. Ionization of  $\sigma$  orbitals (as in **4e**) leads to significant changes in bond angles, whereas in all other cases bond angles remain rather constant. Variations in heavy atom bond lengths upon oxidation or reduction are moderate and very similar in all four series.

In terms of high electron affinities and small reorganization energies, hexaazahexacenes **2f** and **3f** should be the most promising candidates for n-channel semiconducting materials. Taking into account the limited accessibility and stability of hexacenes,<sup>1e,9c,23</sup> however, pentacenes **2e** and **3e** might be more realistic targets for actual device applications. To increase the electron affinities of the latter systems (2.4–2.5 eV) additional

### Chart 3



nitrogens have to be introduced to further lower the LUMO energies. Therefore, we also calculated  $EA$  and  $\lambda_-$  of heptaazapentacenes **5** and **6** that contain two additional nitrogen atoms in the terminal rings (Chart 3).

Structures and properties of **5** and **6** are summarized in Figure 8. Both compounds have electron affinities around 3 eV, whereas the reorganization energies for electron transport are 0.18–0.2 eV, an acceptable range although somewhat higher than  $\lambda_+$  for pentacene **1e**.

Despite the increase in reorganization energy, these compounds have the potential to achieve high mobilities due to very

(22) Whereas the use of small basis sets (without augmentation by diffuse functions) does not lead to strong deviations even for  $\lambda_-$ , the practice in some earlier studies to double one component, instead of calculating both contributions explicitly, is somewhat questionable in view of these results and might lead to systematic errors.

(23) Mondal, R.; Shah, B. K.; Neckers, D. C. *J. Am. Chem. Soc.* **2006**, *128*, 9612 and references given therein.

(24) For example: (a) Allerhand, A.; Schleyer, P. v. R. *J. Am. Chem. Soc.* **1963**, *85*, 175. (b) Desiraju, G. R. *Angew. Chem., Int. Ed. Engl.* **1995**, *34*, 2311. (c) Desiraju, G. R. *Chem. Commun.* **1997**, 1475. (d) Mazik, M.; Blaser, D.; Boese, R. *Tetrahedron* **2001**, *57*, 5791. See also: (e) Desiraju, G. R. *Acc. Chem. Res.* **1991**, *24*, 290. (f) Desiraju, G. R. *Acc. Chem. Res.* **1996**, *29*, 441.

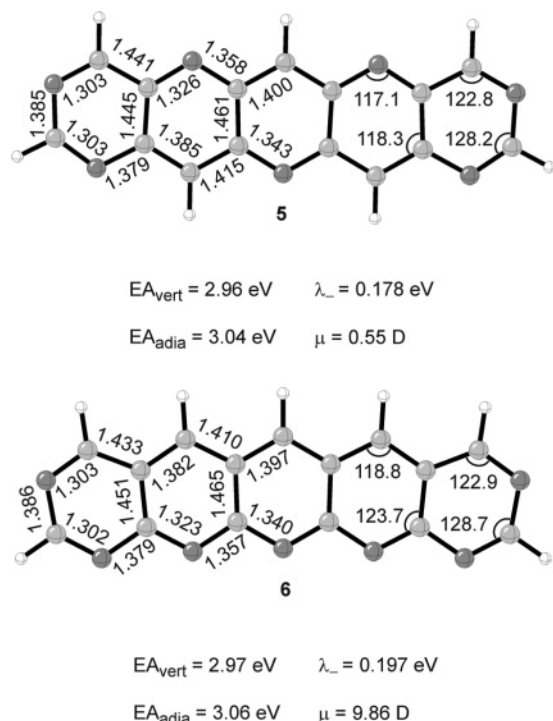
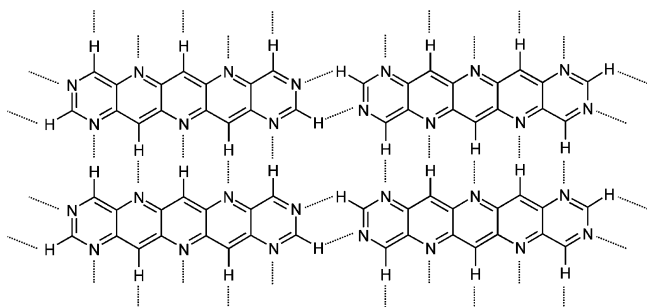


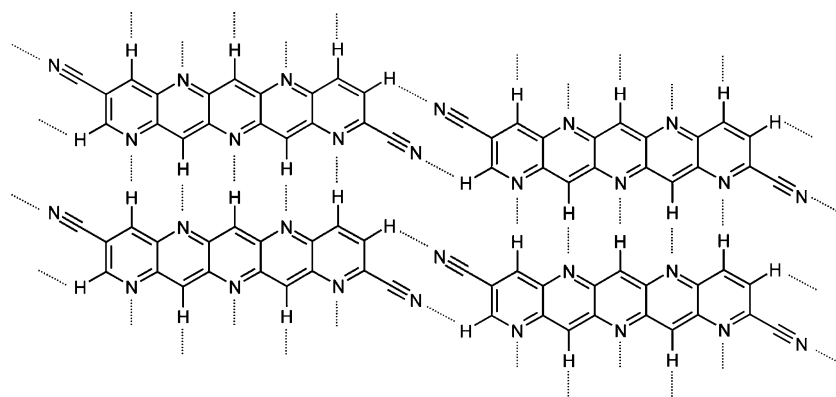
**Figure 8.** Selected structural parameters (bond lengths in Å, angles in deg), electron affinities, reorganization energies, and dipole moments of heptaazapentacenes **5** and **6**.

#### Chart 4



regular cofacial alignments in the solid state. Although CH–N hydrogen bonds are comparatively weak,<sup>24,25</sup> the large number of contacts is expected to facilitate the formation of highly ordered two-dimensional sheets in self-complementary systems (Chart 4). In addition, for both compounds small interlayer distances can be expected, because the sheets can pack in a way where negatively polarized nitrogen atoms of one sheet

#### Chart 5

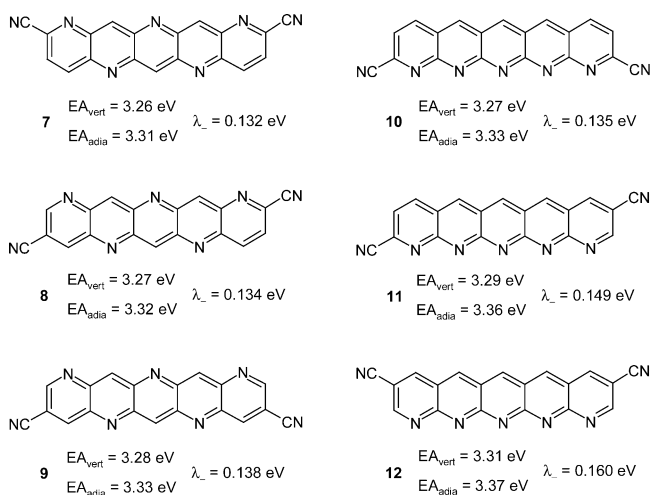


are located over positively polarized C(H) atoms of another. The strong dipole moment of **6** should also contribute to interaction between the sheets.<sup>26</sup> Apart from face-to-face stacking for optimum charge transport, these arrangements should also contribute to the kinetic stability of n-channel semiconductors, because a barrier for diffusion of oxygen or water into the channel region is imposed by dense packing. A detailed understanding how substitution of CH by N in oligoacenes influences the crystal structures of these compounds and how many contacts are required to stabilize a sheet relative to a herringbone structure has to be developed to fully exploit heteroatomic substitution as a versatile principle in acene-based transistor design.

As an alternative to the introduction of additional nitrogen atoms into **2e** or **3e**, electron-withdrawing substituents may be employed to increase the electron affinity of these compounds. Whereas the simplest members of series **2** and **3** still adopt a herringbone structure,<sup>25</sup> it is well-known that 1,4-dicyanobenzene prefers a planar network structure dominated by intermolecular CN–HC interactions.<sup>24b,c,27</sup> Increased mobility and improved air stability have been reported for some perylene bisimide based OTFTs upon cyano substitution in the bay region.<sup>4c</sup> It is thus tempting to investigate dicyano derivatives **7–12**, in which the cyano groups serve as supramolecular synthons<sup>24b,c</sup> to create an additional driving force for  $\pi$ -stacking, as indicated in Chart 5. Electron affinities and reorganization energies of self-complementary dicyanopentacenes are summarized in Chart 6.

The electron affinities of the six isomers are almost identical (3.3 eV) and ideal for semiconductor applications.<sup>1f</sup> Substitution by  $\pi$ -conjugating groups (F, Cl) has been shown to increase the reorganization energies of pentacenes drastically, and this observation has been attributed to the introduction of additional degrees of freedom for structural relaxation upon reduction.<sup>7,8k</sup> It is thus remarkable that all dicyano derivatives **7–12** require somewhat smaller reorganization energies than **2e** and **3e**. Substitution in the ortho position to nitrogen leads to slightly smaller values for  $\lambda_{-}$  than in the meta position, and analogous to the unsubstituted heterocycles, the dicyano derivatives of **2e** require smaller reorganization energies than that of **3e**. The most promising compounds for materials applications in this series are **7–10** that require the smallest reorganization energies for electron transport among all functionalized pentacenes investigated so far.

Chart 6



## Conclusions

A number of nitrogen-substituted oligoacenes containing  $n$ ,  $n + 2$ , or  $2n$  nitrogen atoms has been investigated computationally to elucidate their potential as n-channel semiconducting materials. High electron affinities (3–4 eV) and small reorganization energies are considered to be necessary properties for such compounds. At least seven nitrogen atoms have to be introduced into pentacene to increase the  $EA$  to the required level. Although  $\lambda_{\text{re}}$  increases upon heteroatomic substitution,

(25) For a high-level computational study of pyridine dimers and trimers, see: Piacenca, M.; Grimme, S. *Chem. Phys. Chem.* **2005**, *6*, 1554. The fact that pyridine crystallizes in various phases with different crystal structures has been attributed to the similar energy of several stacked, T-shaped, and hydrogen-bonded complexes.

the overall values for several nitrogen-rich pentacenes are below 0.20 eV. Particularly promising for field effect applications are self-complementary compounds in which a large number of CH–N interactions is expected to change the solid-state structure of pentacenes from a herringbone to a graphite-like sheet structure. Strong interactions between the sheets should furthermore lead to improved air stability of n-channel OTFTs. The introduction of appropriate substituents into the terminal rings offers additional flexibility for fine-tuning the properties of these semiconductors, as discussed for representative dicyano derivatives of **2e** and **3e**. These substituents increase the electron affinity to 3.3 eV, reduce the reorganization energy below 0.14 eV, and also serve as supramolecular synthons to enforce face-to-face alignments. Experimental and computational studies to verify the predictions made in this work are currently in progress in our laboratories.

**Acknowledgment.** We are grateful to the National Science Foundation for financial support and for computational facilities used in this research. M.W. thanks the Alexander von Humboldt Foundation for a Feodor Lynen fellowship.

**Supporting Information Available:** Cartesian coordinates and energies of all calculated structures and the complete citation of ref 13 are available. This material is available free of charge via the Internet at <http://pubs.acs.org>.

JA067087U

- (26) For acenes with strongly electron-withdrawing groups at one end of the molecule, Nuckolls et al. found very compact and  $\pi$ -stacked structures with an alternating arrangement of dipoles in the crystal: (a) Miao, Q.; Lefenfeld, M.; Nguyen, T.-Q.; Siegrist, T.; Kloc, C.; Nuckolls, C. *Adv. Mater.* **2005**, *17*, 407. See also: (b) Moon, H.; Zeis, R.; Borkent, E.-J.; Besnard, C.; Lovinger, A. J.; Siegrist, T.; Kloc, C.; Bao, Z. *J. Am. Chem. Soc.* **2004**, *126*, 15322.
- (27) Guth, H.; Heger, G.; Drück, U. *Z. Kristallogr.* **1982**, *159*, 185.